

Drawing Trees and Cacti with Integer Edge Lengths on a Polynomial-Size Grid

Henry Förster 

Technical University of Munich, Germany

Stephen Kobourov 

Technical University of Munich, Germany

Jacob Miller 

Technical University of Munich, Germany

Johannes Zink 

Technical University of Munich, Germany

Abstract

A strengthened version of Harborth’s well-known conjecture – known as Kleber’s conjecture – states that every planar graph admits a planar straight-line drawing where every edge has integer length and each vertex is restricted to the integer grid. Positive results for Kleber’s conjecture are known for planar 3-regular graphs, for planar graphs that have maximum degree 4, and for planar 3-trees. However, all but one of the existing results are existential and do not provide bounds on the required grid size. In this paper, we provide polynomial-time algorithms for computing crossing-free straight-line drawings of trees and cactus graphs with integer edge lengths and integer vertex position on polynomial-size integer grids.

2012 ACM Subject Classification Mathematics of computing → Trees; Mathematics of computing → Graph algorithms; Theory of computation → Graph algorithms analysis

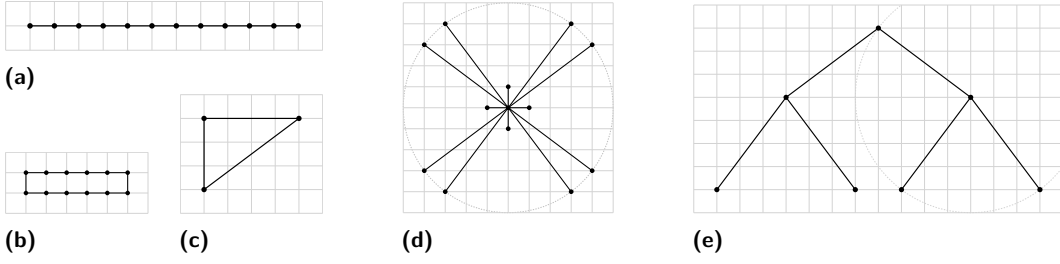
Keywords and phrases Harborth’s conjecture, tree drawings, cactus drawings, integer edge lengths, grid drawings

1 Introduction

Wagner in 1936 [21], Fáry in 1948 [7], and Stein in 1951 [17] proved independently that every planar graph has a crossings-free drawing with edges drawn by straight-line segments. These results are existential and do not lend themselves to algorithms to actually obtain straight-line crossings-free drawing of planar graphs. Later, algorithms that do create such drawings were described by Tutte in 1963 [20], Chiba, Yamanouchi, and Nishizeki in 1984 [5], and Read in 1986 [14]. The underlying difficulty of these algorithms and the generated drawings is that vertex positions are real numbers, rather than integers, and that the ratio between the longest and shortest edge is exponential in the size of the graph. Such drawings are difficult to read as the short edges mean vertices are placed very close to each other.

To draw planar graphs on a computer screen it helps to have vertices at integer coordinates. In 1990, two algorithms for embedding planar graphs on integer grids of size polynomial in the size of the graph appeared. The algorithm of de Fraysseix, Pach and Polack [6] relies on canonical orders whereas Schnyder’s algorithm [15] uses a decomposition of the graph into three trees from which barycentric coordinates can be computed. Both algorithms provide a straight-line drawing on the $\mathcal{O}(n) \times \mathcal{O}(n)$ grid, where n is the number of vertices. Thus, the ratio between the longest and shortest edge is linear rather than exponential, avoiding the problem of unreadable parts where vertices are too close to each other.

Now that we can draw planar graphs with straight-line edges on a (polynomial-size) grid, can we ensure that all edge lengths are integers? The algorithms of de Fraysseix, Pach and Polack [6] and Schnyder [15] can (and indeed do) produce irrational edge lengths, but



■ **Figure 1** Compact truly integral Fáry embeddings of (a) a path on 12 vertices, (b) a cycle on 12 vertices, (c) a cycle on 3 vertices, (d) a star on 13 vertices and (e) a full binary tree of depth 3.

perhaps this can be avoided. Harborth’s conjecture [10, 12] asks whether every planar graph has a crossings-free realization with straight-line segments of integer lengths, referred to as integral Fáry embeddings [4]. A stronger version of Harborth’s conjecture, called Kleber’s conjecture, asks whether an integral Fáry embedding exists where every vertex is located on the integer grid [13]. We will refer to these drawings as *truly integral Fáry embeddings*.

Sun [18] uses rigidity matrices to prove that all planar $(2, 3)$ -sparse graphs admit integral Fáry embeddings. A graph G is (a, b) -sparse if every subgraph G' of G has at most $a|V(G')| - b$ edges. $(2, 3)$ -sparse graphs include series-parallel, outerplanar, and planar bipartite graphs. In 2024, Chang and Sun [4] show this result also for all planar 4-regular graphs, which fixes some problems of a previous attempt [19].

Geelen, Guo, and McKinnon [8] show that every planar max-degree-3 graph admits a truly integral Fáry embedding. Biedl observes that this technique can be applied to all planar $(2, 1)$ -sparse graphs, which include all max-degree-4 graphs that are non-4-regular. Independently, Benediktovich [1] shows this result for max-degree-4 graphs that are non-4-regular and for planar 3-trees.¹ The latter results provide drawings where the vertices have rational coordinates, thus, can be scaled to integers. However, they make use of a theorem by Berry [2] to position vertices on a rational point in an ε -disk around a real point. The application of Berry’s theorem doesn’t provide guarantees on the distance towards an integral point. Thus, if we were to scale the drawing to provide a truly integral Fáry embedding, no bound on the area can be provided.

Biedl [3] shows how to draw planar max-degree-3 graphs with integer edge lengths and integer coordinates. She employs an algorithm by Kant [11] from 1992 for drawing 3-connected 3-regular graphs on the hexagonal grid. Then, the drawing is skewed such that the three resulting slopes are part of Pythagorean triples (see below). Non-3-connected parts are drawn independently, scaled and glued. Note that the latter step may require a large grid size.

To the best of our knowledge, the algorithm by Biedl [3] that produces, for 3-connected 3-regular planar graphs, truly integral Fáry embeddings on a quadratic-size grid is the only algorithm in the literature that provides a polynomial upper bound on the area.

Our contribution. In this paper, we consider the practical question about the grid size of truly integral Fáry embeddings; see Figure 1 for a few examples. Specifically, we show that trees and cactus graphs admit truly integral Fáry embeddings on an $\mathcal{O}(n^2) \times \mathcal{O}(n^2)$ and $\mathcal{O}(n^3) \times \mathcal{O}(n^3)$ integer grids, respectively. In special cases, we achieve better bounds –

¹ Essentially, for planar 3-trees, it has also been shown by Kemnitz and Harborth [12] before.

namely, for stars, binary trees and trees of depth d , we achieve $\Theta(n^2)$, $\mathcal{O}(n^2)$ and $\mathcal{O}(n^2 d^2)$ area, respectively. Our proofs are constructive and correspond to efficient algorithms. We analyze the precise constant factors of the grid area occupied by our drawings.

2 Preliminaries

The existence of Pythagorean triples is among the oldest observations in mathematics, predating even Euclid. Their algebraic definition and connection to geometry are likely some of the first non-trivial proofs shown to elementary and primary school students. They are defined as all triples of integers a, b, c which satisfy the equation $a^2 + b^2 = c^2$. These triples are exactly the side lengths of right-angled triangles with integer side lengths. In this section, we review a few properties of Pythagorean triples. For the convenience of the reader we provide explicit proofs for most of the statements.

To ensure integer edge lengths on an integer grid, we are restricted to using Pythagorean triples. This is easy to observe; the length of any line segment from (x_1, y_1) to (x_2, y_2) is given by the Euclidean distance $\sqrt{(x_2 - x_1)^2 + (y_2 - y_1)^2}$. This length can only be integer when the sum of square differences in the coordinates is square. In particular, if we enforce that the endpoints of the line segment are integer, then the difference in x coordinate, the difference in y coordinate, and the length ℓ of the segment form a Pythagorean triple (x, y, ℓ) .

If a triple a, b, c is a Pythagorean triple, then so is ka, kb, kc for any positive integer k . A triple is called *primitive* if there is no integer $k > 1$ that divides a, b , and c evenly; that is a, b , and c are coprime. We leverage that each primitive Pythagorean triple forms a triangle with a unique (clock-wise) sequence of internal angles. In particular for a given (primitive) Pythagorean triple (x, y, ℓ) , if a vertex u is located at point $(p_x, p_y) \in \mathbb{N}^2$ and has an edge to a not-yet-placed vertex v , then placing vertex v at $(p_x + x, p_y + y)$ guarantees both integer coordinates for v and integer edge length ℓ for the edge uv . If u is adjacent to another vertex w , then using a different primitive Pythagorean triple guarantees, due to the different angles, that the edges uv and uw do not overlap. Our algorithms rely on the algorithmic generation of triples. To this end, we will rely on a generator referred to as *Euclid's formula* (see, e.g., [16]):

► **Lemma 1.** *Let $m, n \in \mathbb{N}_{\geq 0}$. Then, the triple (x, y, ℓ) with*

$$x = m^2 - n^2, \quad y = 2mn, \quad \ell = m^2 + n^2 \tag{1}$$

is a Pythagorean triple.

Proof. Since m and n are integer, so are x, y and ℓ . Moreover, $x^2 + y^2 = (m^4 - 2m^2n^2 + n^4) + (4m^2n^2) = (m^4 + 2m^2n^2 + n^4) = \ell^2$. ◀

We next assure that we can generate all primitive Pythagorean triples using Euclid's formula. The following theorem has been shown for instance in [16, Theorem 1].

► **Theorem 2 ([16]).** *Let $P = (x, y, \ell)$ be a primitive Pythagorean triple such that y is even. Then, there are $m, n \in \mathbb{N}_{\geq 0}$ such that P is generated using Equation (1).*

One may now wonder what happens if y is odd. According to Theorem 2, the following generator generates all primitive Pythagorean triples where x is even for $m, n \in \mathbb{N}_{\geq 0}$:

$$x = 2mn, \quad y = m^2 - n^2, \quad \ell = m^2 + n^2 \tag{1'}$$

Moreover, the following lemma establishes that (1) and (1') are indeed sufficient to generate all primitive Pythagorean triples. This may be concluded from the observation

that x and y must be co-prime [16, 1.5]; here, we provide an explicit proof for the following special case of the statement.

► **Lemma 3.** *In any primitive Pythagorean triple (a, b, c) , exactly one of a and b is odd.*

Proof. First, assume for a contradiction that both a and b are even, i.e., $a = 2i$ and $b = 2j$ for $i, j \in \mathbb{N}_{\geq 0}$. Then, also c is even, i.e., $c = 2k$ for $k \in \mathbb{N}_{\geq 0}$. But then $(i, j, k) = (\frac{a}{2}, \frac{b}{2}, \frac{c}{2})$ is Pythagorean triple; a contradiction to the fact that (a, b, c) is primitive.

Second, assume for a contradiction that both a and b are odd, i.e., $a = 2i + 1$ and $b = 2j + 1$ for $i, j \in \mathbb{N}_{\geq 0}$. Then, a^2 and b^2 are also odd as they are the product of two odd numbers and c^2 must be even as it is the sum of two odd numbers. Hence, also c must be even, i.e., $c = 2k$ for $k \in \mathbb{N}_{\geq 0}$. But then:

$$\begin{aligned} a^2 + b^2 &= c^2 \\ \Leftrightarrow (2i + 1)^2 + (2j + 1)^2 &= (2k)^2 \\ \Leftrightarrow 4i^2 + 4i + 1 + 4j^2 + 4j + 1 &= 4k^2 \\ \Leftrightarrow 4(i^2 + i + j^2 + j) + 2 &= 4k^2 \\ \Leftrightarrow (i^2 + i + j^2 + j) + \frac{1}{2} &= k^2 \end{aligned} \tag{2}$$

The left-hand side of (2) contains the term $(i^2 + i + j^2 + j)$ which is a natural number as $i, j \in \mathbb{N}$. Thus, $(i^2 + i + j^2 + j) + \frac{1}{2} \notin \mathbb{N}$. On the other hand, $k^2 \in \mathbb{N}$; a contradiction. ◀

Theorem 2 and Lemma 3 immediately imply the following:

► **Corollary 4.** *Let $P = (x, y, \ell)$ be any primitive Pythagorean triple. Then, there are $m, n \in \mathbb{N}_{\geq 0}$ such that P is generated using Equation (1) or (1').*

Equations (1) and (1') provide us with a possibility to generate the Pythagorean triples required by our algorithms. For our algorithmic results, we are on the other hand also interested in the size of values x , y and ℓ of Pythagorean triple (x, y, ℓ) as these will influence the required area and running time. A preliminary review of the growth of Pythagorean triples for smaller values of x , y and ℓ can for instance be found in [16, 2.7 and Chapter 3]. Here, we are interested in bounding the asymptotic growth. To this end, we will provide a complete proofs as we are not aware of literature explicitly discussing it (despite it following from combining some easy observations with known results on the Farey sequence).

We first observe the following:

► **Lemma 5.** *Let $m, n, a, b, k \in \mathbb{N}_+$ such that $m > n$, $a > b$ and*

$$m^2 - n^2 = k(a^2 - b^2) \tag{3}$$

$$2mn = k(2ab) \tag{4}$$

$$m^2 + n^2 = k(a^2 + b^2). \tag{5}$$

Then:

$$\frac{m}{n} = \frac{a}{b} \tag{6}$$

Proof. We begin by calculating the sum of (3) and (5):

$$m^2 - n^2 + m^2 + n^2 = k(a^2 - b^2) + k(a^2 + b^2) \Leftrightarrow 2m^2 = 2ka^2 \Leftrightarrow k = \frac{m^2}{a^2} \tag{7}$$

Next, we compute the difference between (5) and (3):

$$m^2 + n^2 - (m^2 - n^2) = k(a^2 + b^2) - k(a^2 - b^2) \Leftrightarrow 2n^2 = 2kb^2 \Leftrightarrow k = \frac{n^2}{b^2} \quad (8)$$

Both (7) and (8) provide a description of k which we can set equal:

$$\frac{m^2}{a^2} = k = \frac{n^2}{b^2} \Leftrightarrow \frac{m^2}{n^2} = \frac{a^2}{b^2} \Leftrightarrow \left(\frac{m}{n}\right)^2 = \left(\frac{a}{b}\right)^2 \quad (9)$$

Since $m, n, a, b \geq 1$, Equation (9) implies (6) which concludes the proof. \blacktriangleleft

Next, we define an ordering \prec_{prim} of the primitive Pythagorean triples. We only consider Pythagorean triples (x, y, ℓ) where $x, y, \ell > 0$. Note that this triples are generated by Equations (1) and (1') when $m > n > 0$. Let $P = (x, y, \ell)$ and $P' = (x', y', \ell')$ be two primitive Pythagorean triples with $P \neq P'$ and $x, x', y, y', \ell, \ell' > 0$. By Corollary 4, there are integers $m, n \in \mathbb{N}_+$ such that P is generated when inserting m and n into Equation (1) or (1') and there are integers $m', n' \in \mathbb{N}_+$ such that P' is generated when inserting m' and n' into Equation (1) or (1'). Note that $m > n$ as $\ell > 0$. We now say that $P \prec_{\text{prim}} P'$ if and only if one of the following applies: **1.** $m < m'$, **2.** $m = m'$ and $n < n'$, or, **3.** $m = m'$, $n = n'$ and P is generated using Equation (1) (i.e., P' is generated using (1')).

Observe that \prec_{prim} defines a total ordering of the primitive Pythagorean triples. Hence, in the following, let $\mathcal{P} = (P_1, P_2, \dots)$ denote the set of Pythagorean triples ordered with respect to \prec_{prim} , i.e., for $P_i, P_j \in \mathcal{P}$, we have $P_i \prec_{\text{prim}} P_j$ if and only if $i < j$. Moreover, we say that P_i is the i -th primitive Pythagorean triple and that $\mathcal{P}_k = (P_1, \dots, P_k) \subset \mathcal{P}$ is the set of the first k primitive Pythagorean triples. Using Lemma 5, we can bound the numerical values x_k, y_k and ℓ_k in $P_k = (x_k, y_k, \ell_k)$:

► Lemma 6. *Let $P_k = (x_k, y_k, \ell_k) \in \mathcal{P}$ be the k -th Pythagorean triple generated by inserting m and n into Equation (1) or (1'). Then, $m, n \leq \frac{\pi}{\sqrt{3}}\sqrt{k} \in \mathcal{O}(\sqrt{k})$ and $x_k, y_k, \ell_k \leq \frac{2\pi^2}{3}k \in \mathcal{O}(k)$. Moreover, for sufficiently large k , we have $m > \left(\frac{\pi}{\sqrt{3}} - 1\right) \cdot \sqrt{k} \in \Omega(\sqrt{k})$ and $x_k, y_k, \ell_k > 2\left(\frac{\pi}{\sqrt{3}}\right)^2 \cdot k \in \Omega(k)$.*

Proof. According to Lemma 5, we can obtain two primitive Pythagorean triples for each irreducible fraction $\frac{m}{n}$ and using numerator m and denominator n as input for Equation (1) and (1'), respectively. The sequence (sorted by value) of irreducible fractions $\frac{m}{n}$ where $0 \leq m, n \leq x$ is known as the Farey sequence \mathcal{F}_x of order x [9, Chapter 4.9]. It is known that

$$|\mathcal{F}_x| = \frac{3}{\pi^2}x^2 + f(x) \quad \text{where } f(x) = \mathcal{O}(x \log x) \text{ and } f(x) \geq 0. \quad [9, \text{Chapter 9.3}]$$

In particular, for $x = \frac{\pi}{\sqrt{3}}\sqrt{k}$, we obtain:

$$|\mathcal{F}_x| \geq \frac{3}{\pi^2} \left(\frac{\pi}{\sqrt{3}}\sqrt{k} \right)^2 = \frac{3\pi^2}{\pi^2 3}k = k$$

Hence, $m, n \leq \frac{\pi}{\sqrt{3}}\sqrt{k}$ and thus $x_k, y_k, \ell_k \leq \frac{2\pi^2}{3}k$.

In contrast, if we choose $x = \left(\frac{\pi}{\sqrt{3}} - 1\right) \sqrt{k}$, we obtain

$$\begin{aligned} |\mathcal{F}_x| &= \frac{3}{\pi^2} \left(\left(\frac{\pi}{\sqrt{3}} - 1 \right) \sqrt{k} \right)^2 + \mathcal{O} \left(\sqrt{k} \log \left(\sqrt{k} \right) \right) \\ &= \left(\frac{3\pi^2}{\pi^2 3} - \frac{6\pi}{\sqrt{3}\pi^2} + 1 \right) \cdot k + \mathcal{O} \left(\sqrt{k} \log \left(\sqrt{k} \right) \right) \\ &= k - \mathcal{O}(k) + \mathcal{O} \left(\sqrt{k} \log \left(\sqrt{k} \right) \right) < k, \end{aligned}$$

i.e., we must have $m > \left(\frac{\pi}{\sqrt{3}} - 1\right) \cdot \sqrt{k}$ for sufficiently large k . \blacktriangleleft

Given Lemma 6, it is now straight-forward to compute the first k Pythagorean triples:

► **Lemma 7.** *The first k Pythagorean triples \mathcal{P}_k can be computed in $\mathcal{O}(k^{3/2})$ time.*

Proof. According to Lemma 6, there is a value $x = \mathcal{O}(\sqrt{k})$, so that each $P \in \mathcal{P}_k$ can be generated by inserting values m and n into Equation (1) or (1') where $m, n \leq x$. Thus, we can iterate over all x^2 possible combinations of values for m and n and check for each generated Pythagorean triple if it is primitive. The primitivity check can be trivially implemented in $\mathcal{O}(\sqrt{k})$ time by testing all possible common divisors. \blacktriangleleft

In our algorithms, the primitive Pythagorean triples are used to decide how to draw edges. Namely, having a primitive Pythagorean triple (x, y, ℓ) , the two endpoints of an edge e will be x units horizontally and y units vertically apart whereas e has length ℓ . To maintain planarity, it will be important to have a sorting of the edges by slope. The *angle* $\alpha(P)$ of a Pythagorean triple $P = (x, y, \ell)$ is equal to $\arctan(\frac{y}{x})$, i.e., it is the angle in the right-angled triangle spanned by edges of lengths x , y , and ℓ that occurs between the edges of lengths x and ℓ . For Pythagorean triples P and P' , we say that $P \prec_{\text{angle}} P'$ if and only if $\alpha(P) < \alpha(P')$. Observe that, due to the definition of the arctan, all angles that correspond to primitive Pythagorean triples of \mathcal{P} are distinct and, hence, \prec_{angle} defines a total ordering of \mathcal{P} . In the following, we denote by $\mathcal{P}_k^\circ = (P_1^\circ, \dots, P_k^\circ)$ the *angle-sorted* first k primitive Pythagorean triples, that is, the permutation of \mathcal{P}_k so that for $P_i^\circ, P_j^\circ \in \mathcal{P}_k^\circ$ we have $P_i^\circ \prec_{\text{angle}} P_j^\circ$.

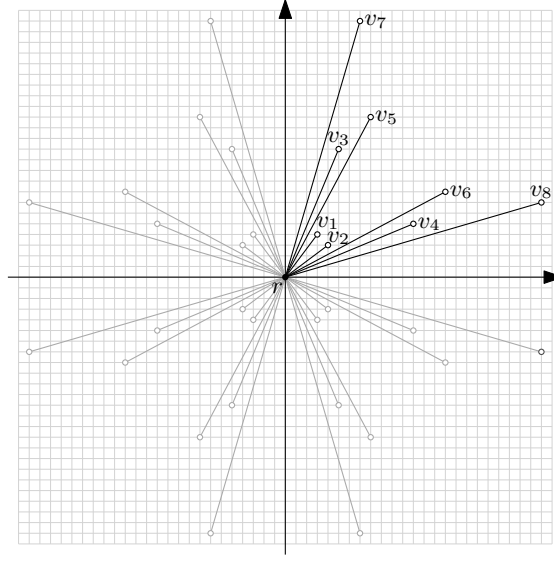
3 Polynomial-Area Truly Integral Fáry Drawings for Trees and Cacti

We show that truly integral Fáry drawings on a polynomial-size grid exist for cacti. For the convenience of the reader, we do not show our main result for cacti directly, but start with some special cases. The result on binary trees is a consequence of the work by Biedl [3], for stars, trees, and cacti we show in three steps how to find and assign suitable primitive Pythagorean triples for drawing such graphs and what size of a grid is used for the drawings.

3.1 Binary Trees

We begin by considering the family of binary trees or, equivalently, subcubic trees. For this family of trees, we show that it is always possible to compute a quadratic area truly integral Fáry embedding. The following statement can be seen as a corollary of Biedl's [3] result for truly integral Fáry drawings of 3-connected 3-regular graph. We essentially, make all non-leaf vertices have degree 3 and then construct the Halin graph being 3-connected and 3-regular.

► **Theorem 8.** *Let $T = (V, E)$ be a binary tree with n vertices. There is a truly integral Fáry embedding on a grid of size $\mathcal{O}(n) \times \mathcal{O}(n)$, which can be found in $\mathcal{O}(n)$ time.*



■ **Figure 2** Drawing of a star T with 32 leaves created with our algorithm in the proof of [Theorem 9](#).

Proof. If T is rooted and directed, we ignore the root and consider the underlying undirected graph. Augment T by adding leaves such that every non-leaf vertex has degree three. Call the resulting subcubic tree T' . Note that T' has fewer than twice as many vertices as T .

Fix any plane embedding of T' and insert a crossing-free cycle C through all its leaves yielding graph G_T , which is a so-called Halin graph. G_T has as many vertices as T' and is a 3-regular graph. Clearly, G_T is 3-connected: for every pair of vertices (u, v) , there is a unique simple path P_1 between u and v only using edges of T' and two simple disjoint paths P_2 and P_3 connecting u and v via C and not using vertices of P_1 , where P_2 traverses C in clockwise and P_3 traverses C in counterclockwise order. We now apply a result by Biedl [3] that states that any 3-connected 3-regular planar graph G – in particular, G_T – admits a truly integral Fáry embedding in $5(N - 2) \times 24(N - 2)$ where N is the number of vertices in G . Since $N \in \mathcal{O}(n)$ in G_T and T is a subgraph of G_T , the statement follows. ◀

3.2 Stars

In the remainder of this section, in a three-step approach, we apply the knowledge about primitive Pythagorean triples first to stars, then to arbitrary trees, and finally to cacti. While in contrast to binary trees, general stars have arbitrary maximum degree, we are again able to yield quadratic area truly integral Fáry embeddings. Here, we begin with stars, for which we use the primitive Pythagorean triples.

► **Theorem 9.** *Let $T = (V, E)$ be a star with n vertices. There is a truly integral Fáry embedding on a grid of size $\left(\frac{\pi^2}{3}n + \mathcal{O}(1)\right) \times \left(\frac{\pi^2}{3}n + \mathcal{O}(1)\right) \approx 3.29n \times 3.29n$, which can be found in $\mathcal{O}(n^{3/2})$ time. Any truly integral Fáry embedding of T needs a grid of size $\Omega(n) \times \Omega(n)$.*

Proof. We describe how to draw T such that every vertex is on a grid point and every edge has integer length. The realization as a linear-time algorithm is straightforward except for determining $\mathcal{O}(n)$ Pythagorean triples, which can be done in $\mathcal{O}(n^{3/2})$ time according to [Lemma 7](#). Place the central vertex r at $(0, 0)$. Label the leaves (arbitrarily or in a given rotation order) v_1, v_2, \dots, v_n . For $i \in \{1, \dots, \lceil (n-1)/4 \rceil\}$, place v_i onto (x_i, y_i) where

(x_i, y_i, ℓ_i) is the i -th primitive Pythagorean triple from \mathcal{P}° . Clearly, each edge rv_i has an integral length ℓ_i and no pair of edges overlaps. So far, we have drawn at least one fourth of the edges in the top right quadrant. Similarly, repeat this process for the other three fourths of edges – for each of them in one of the three remaining quadrants with the same set of primitive Pythagorean triples; see Figure 2.

The resulting drawing is a truly integral Fáry embedding. We next analyze the grid size. By Lemma 6, $x_k, y_k \leq 2\pi^2/3k$. Since $\lceil (n-1)/4 \rceil \leq (n+2)/4$, the maximum x- and y-coordinate is at most $2\pi^2(n+2)/12$ and the minimum x- and y-coordinate is at least $-2\pi^2(n+2)/12$. This yields a grid of size at most

$$\left(2 \cdot \frac{2\pi^2(n+2)}{12} + 1\right) \times \left(2 \cdot \frac{2\pi^2(n+2)}{12} + 1\right) = \frac{\pi^2(n+2)+3}{3} \times \frac{\pi^2(n+2)+3}{3}.$$

Finally, let us argue about the lower bound. Any drawing of a star requires $(n-1)/4$ distinct primitive Pythagorean triples. By Corollary 4, we know that, the generator formulas (1) and (1') generate all primitive Pythagorean triples. Let M and N be the two numbers of these generator formulas with $M > N$. By Lemma 6, to generate $\Theta(n)$ primitive Pythagorean triples, some $M \in \Omega(\sqrt{n})$. We need $\Theta(n)$ distinct pairs of M and N . Hence, if some $M \in \Theta(f(n))$ for some function $f(n) \in \Omega(\sqrt{n})$, then there is a corresponding $N \in \Omega(n/f(n))$. In the generator formulas, this yield $2MN \in \Omega(n)$ and $M^2 - N^2 \in \Theta(f^2(n)) \subseteq \Omega(\sqrt{n}^2) = \Omega(n)$. This corresponds to a grid of size $\Omega(n) \times \Omega(n)$. ◀

We remark that the star drawings are not only asymptotically optimal, but also optimal with respect to the constant factors since we use the smallest primitive Pythagorean triples. No other approach is possible besides using larger, suboptimal Pythagorean triples.

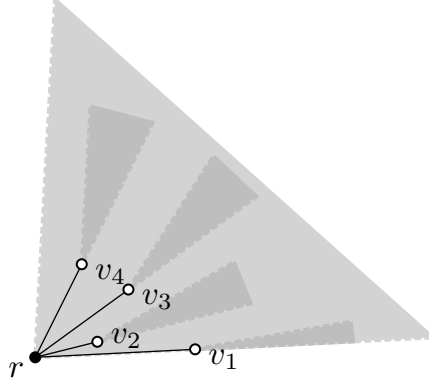
3.3 Arbitrary Trees

Next, we essentially generalize our algorithm for stars to arbitrary trees at the cost of a factor d where d is the depth of the tree.

Let $T = (V, E)$ be a (rooted) tree, which has n vertices, t leaves, and depth d . In the following, we describe an algorithm that computes a truly integral Fáry embedding on a grid of size $\frac{2\pi^2}{3}td \times \frac{2\pi^2}{3}td \subseteq \mathcal{O}(n^2) \times \mathcal{O}(n^2)$ in $\mathcal{O}(n + t^{3/2})$ time.

Notation for general trees. Denote the root of T by r . If no root is given, pick r arbitrarily, e.g., by choosing the vertex with greatest graph centrality. Assume that we are given an order of the children at each vertex, i.e., a rotation system. If no rotation system is given, choose it arbitrarily. For a vertex $v \in V$, we denote by T_v the subtree of T rooted at vertex v , by $d(T_v)$ the depth of T_v and by $L(T_v)$ the number of leaves in T_v ; e.g., $T_r = T$, $d(T_r) = d$, $L(T_r) = t$, and $T_v = (\{v\}, \emptyset)$, $d(T_v) = 0$ and $L(T_v) = 1$ if v is a leaf. Next, we describe how to generate a truly integral Fáry embedding of T . The realization as a linear-time algorithm is straight-forward, however, we add $\mathcal{O}(t^{3/2})$ additional running time for computing $\mathcal{O}(t)$ primitive Pythagorean triples; see Lemma 7.

Algorithm. Similar to stars, we will place r at $(0, 0)$ and we will use t primitive Pythagorean triples for drawing T . Here, for simplicity we only use the first quadrant. Assign the first child v_1 of r the first $L(T_{v_1})$ primitive Pythagorean triples from \mathcal{P}_t° , assign the second child v_2 of r the next $L(T_{v_2})$ primitive Pythagorean triples from \mathcal{P}_t° , etc. Draw each child v of r at the coordinates (x, y) where (x, y, ℓ) is the first primitive Pythagorean triple among $\mathcal{P}(v)$, where $\mathcal{P}(v)$ is the set of primitive Pythagorean triples assigned to v , sorted as in \mathcal{P}_t° . For



■ **Figure 3** Schematization of our recursive drawing algorithm in [Section 3.3](#): Vertex r is placed at $(0, 0)$ and its subtree is drawn inside the light-gray cone according to [Invariant 2](#). Each child v_i is assigned an exclusive set of slopes (defined by $\mathcal{P}(v_i)$) resulting in the non-overlapping gray cones centered at the child components. The edge between r and v_i is drawn using the first triple assigned to v_i .

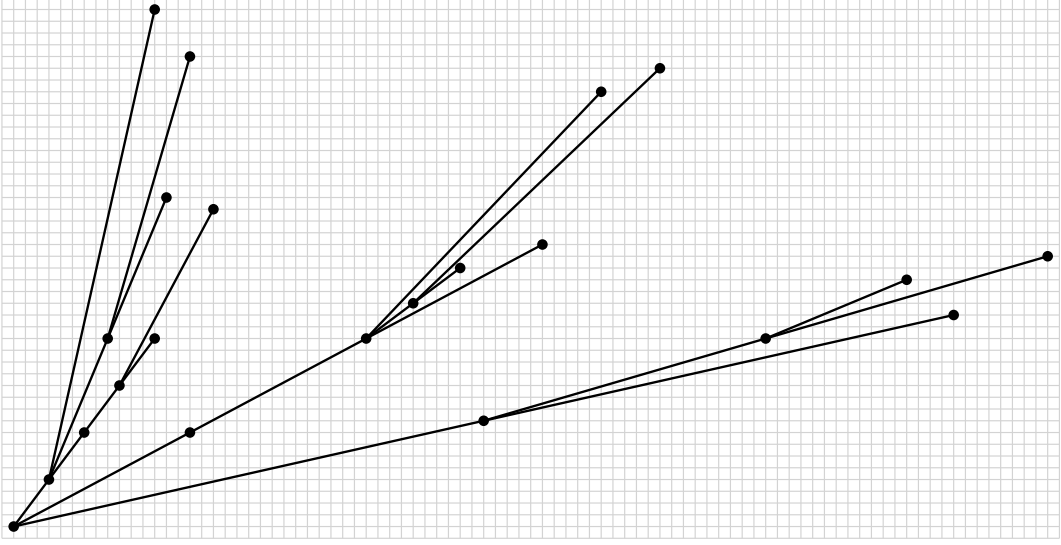
each child v of r , for which v is not a leaf of T , we draw the subtree T_v recursively: in the recursive call, we assume that the coordinate system is centered at the position of v and we use exactly the primitive Pythagorean triples assigned to v ; see [Figure 3](#).

Correctness. We next show that for every vertex v of T , the following invariants hold:

1. The drawing of T_v is a truly integral Fáry embedding.
2. The drawing of T_v lies in a cone that is rooted at v and bounded by two rays emanating at v and having slopes y_1/x_1 and $y_{L(T_v)}/x_{L(T_v)}$, where the triples (x_1, y_1, ℓ_1) and $(x_{L(T_v)}, y_{L(T_v)}, \ell_{L(T_v)})$ denote the first and the last Pythagorean triple of $\mathcal{P}(v)$, respectively. See also the gray cones in [Figure 3](#) for an illustration.
3. In the drawing of T_v , the Euclidean distance between v and any vertex of T_v is at most $d(T_v) \cdot \frac{2\pi^2}{3} \cdot t$.

Base Case: A leaf. We start with the base case that v is a leaf. The drawing of T_v contains only v being placed at $(0, 0)$. Trivially, [Invariants 1–3](#) hold.

Recursion: Combining child components of a vertex u . We consider the combination step where u is the root of T_u and u has children v_1, \dots, v_k for some $k \in \{1, \dots, n-1\}$. We assume that T_{v_1}, \dots, T_{v_k} are drawn according to [Invariants 1–3](#). We place u at $(0, 0)$ and, for each $i \in \{1, \dots, k\}$, we place the drawing of T_{v_i} such that v_i lies on (x, y) where (x, y, ℓ) is the first primitive Pythagorean triple of $\mathcal{P}(v_i)$. This is a translation of T_{v_i} from a grid point to another grid point; see also the child components of r in [Figure 3](#). All vertices of T_{v_i} as well as u lie on grid points and all edges of T_u have integer length. Clearly, there is no crossing among the edges uv_1, \dots, uv_k . Suppose for a contradiction that for some $i, j \in \{1, \dots, k\}$, $i < j$, the drawings of T_{v_i} and T_{v_j} intersect. By [Invariant 2](#), this implies that the cones of T_{v_i} and T_{v_j} intersect. Since $i < j$, uv_i has a smaller slope than uv_j . For the cone based in v_i to intersect the cone based in v_j , the upper bounding ray of v_i 's cone must have a greater slope than the lower bounding ray of v_j 's cone. However, all Pythagorean triples contained in $\mathcal{P}(v_i)$ correspond to smaller slopes than the Pythagorean triples contained in $\mathcal{P}(v_j)$ since they are sorted by angle. A similar argument can be made to show that none of the edges



■ **Figure 4** Example output of our algorithm for general trees.

uv_1, \dots, uv_k crosses T_{v_1}, \dots, T_{v_k} . Hence, the combined drawing is planar and [Invariant 1](#) is satisfied. Furthermore, consider the rays emanating from u with the slopes corresponding to the first and the last Pythagorean triple of $\mathcal{P}(u)$. They contain all edges uv_1, \dots, uv_k and the cones based at v_1, \dots, v_k . Therefore, [Invariant 2](#) is satisfied. Finally, the maximum Euclidean distances between u and any of v_1, \dots, v_k is $\frac{2\pi^2}{3}t$ by [Lemma 6](#). Together with [Invariant 3](#) and the triangle inequality, this implies that the Euclidean distance between u and any vertex x in T_{v_1}, \dots, T_{v_k} is

$$\text{dist}(u, x) \leq \frac{2\pi^2}{3}t + \max_{i=1}^k d(T_{v_i}) \cdot \frac{2\pi^2}{3}t = \left(\max_{i=1}^k d(T_{v_i}) + 1 \right) \frac{2\pi^2}{3}t = d(T_u) \frac{2\pi^2}{3}t.$$

This satisfies [Invariant 3](#).

[Invariants 1–3](#) for the root r imply the following theorem.

► **Theorem 10.** *Let $T = (V, E)$ be a (rooted) tree, which has n vertices, t leaves, and depth d . There is a truly integral Fáry embedding on a grid of size $\frac{2\pi^2}{3}td \times \frac{2\pi^2}{3}td \subseteq \mathcal{O}(n^2) \times \mathcal{O}(n^2)$, which can be found in $\mathcal{O}(n + t^{3/2})$ time.*

See [Figure 4](#) for an example output of our algorithm. We remark that by using all quadrants (and not just the first one) similar to [Theorem 9](#), we can reduce the grid size even to $(\pi^2td/3 + \mathcal{O}(1)) \times (\pi^2td/3 + \mathcal{O}(1)) \approx 3.29td \times 3.29td$. *Balanced trees* are those trees that have depth $\mathcal{O}(\log n)$. They are relevant for many practical applications. By [Theorem 10](#), they can be drawn on a grid of size $\mathcal{O}(n \log n) \times \mathcal{O}(n \log n)$.

3.4 Cacti

We extend the algorithm from [Section 3.3](#) to work for cacti. A *cactus graph* is a 1-vertex-connected graph such that each 2-vertex-connected component is either a cycle or a single edge; i.e., trees are cacti where every 2-vertex-connected component is a single edge.

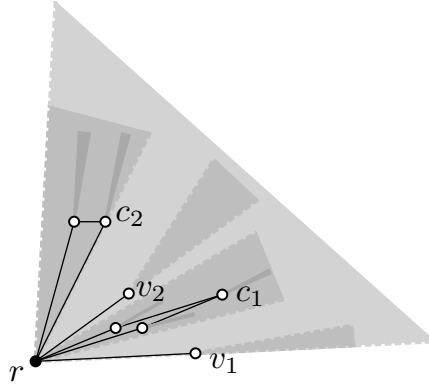
Notation for cacti. Let $C = (V, E)$ denote a cactus with diameter d , t leaves, o cycles and δ 3-cycles. Further, let $r \in V$ be any vertex of C called the *root*, e.g., the one with greatest

graph centrality. In the following, we assume that C is associated with an outerplane rotation system and that each edge (u, v) is oriented so that u is closer to r than v , or they are equally close to r . Note that the orientation can be computed using a BFS traversal rooted at r . While in trees, we have constructed drawings for the subgraphs rooted at *each* vertex, here, we decompose the graph at *cut-vertices*, i.e., vertices whose removal separates C . As in trees we call a vertex v a *leaf* if it is a degree-1 vertex without successors. For a cycle c in C , we call the unique vertex s_c on c with no predecessor on c the *origin* of cycle c . In addition, we call the unique vertex t_c on c with no successor on c the *terminal* of cycle c . The edges on c can be separated in two directed paths, the *left path* $p_{\leftarrow}(c)$ and the *right path* $p_{\rightarrow}(c)$ where the first edge of the left path precedes the first edge of the right path in a clockwise sorting of the edges incident to s_c . We assume, w.l.o.g., that $|p_{\leftarrow}(c)| \in \{|p_{\rightarrow}(c)|, |p_{\rightarrow}(c)| + 1\}$, i.e., if the left and right paths differ in length, then the left path is longer. We say that a cycle c (or an edge e) is a *child* of a vertex v if v is the origin of c (or source of e , respectively).

For a cut-vertex, the root, or a leaf v denote by C_v the subcactus of C rooted at v , i.e., the subgraph induced by all vertices reachable from v via directed edges. Moreover, we denote by $d(C_v)$ the diameter of C_v , by $L(C_v)$, the number of leaves in C_v , by $O(C_v)$ the number of cycles in C_v . Moreover, we denote by $\Delta(C_v)$ the number of 3-cycles in C_v . For example, if v is the root r , then $C_r = C$, $d(C_r) = d$, $L(C_r) = t$, $O(C_r) = o$, $\Delta(C_r) = \delta$. If v is a leaf, then $C_v = (\{v\}, \emptyset)$, $d(C_v) = 0$ and $L(C_v) = 1$, $O(C_v) = \Delta(C_v) = 0$. If v is the origin of a single cycle c such that no vertex on c except v has a child, then $C_v = (V[c], E[c])$, $d(C_v) = \lfloor V[c]/2 \rfloor$, $L(C_v) = 0$, $O(C_v) = 1$, and $\Delta(C_v) = 1$ if c is a 3-cycle or $\Delta(C_v) = 0$ otherwise. We define the same parameters for cycles: For a cycle c with origin v , let C_c denote the subgraph of C induced by $V[c]$ and all vertices reachable via a directed path that starts at a vertex on c other than v . Again, we denote by $d(C_c)$ the diameter of C_c , by $L(C_c)$, the number of leaves in C_c , by $O(C_c)$ the number of cycles in C_c and by $\Delta(C_c)$ the number of 3-cycles in C_c . Moreover, we denote by $L_{\leftarrow}(C_c)$, $O_{\leftarrow}(C_c)$, and $\Delta_{\leftarrow}(C_c)$ the number of leaves, cycles, and 3-cycles, resp., in the subcacti rooted at internal vertices along $p_{\leftarrow}(c)$ or t_c . Similarly, we denote by $L_{\rightarrow}(C_c)$, $O_{\rightarrow}(C_c)$, and $\Delta_{\rightarrow}(C_c)$ the number of leaves, cycles, and 3-cycles, resp., in the subcacti rooted at internal vertices along $p_{\rightarrow}(c)$ (excluding t_c).

Algorithm. Similar to the previous two algorithms, the following algorithm straightforwardly admits a linear-time implementation except for the step of computing the primitive Pythagorean triples. Again, we place r at $(0, 0)$ and we use at most $t + 2o$ primitive Pythagorean triples for drawing T . As in the algorithm for arbitrary trees, we restrict ourselves to the first quadrant. Let $\mathcal{C}_r = c_1, \dots, c_i$ denote the child cycles with origin r and let $\mathcal{V}_r = v_1, \dots, v_j$ denote the child vertices of r . Since C is associated with an outerplane rotation system \mathcal{E} , the successor set $\mathcal{S}_r = \mathcal{C}_r \cup \mathcal{V}_r$ is well-ordered with respect to \mathcal{E} . We assign the first successor $s_1 \in \mathcal{S}_r$ the first $L(C_{s_1}) + 2O(C_{s_1})$ primitive Pythagorean triples $\mathcal{P}_{s_1}^\circ$ from \mathcal{P}_{t+2o}° , the second successor $s_2 \in \mathcal{S}_r$ the next $L(C_{s_2}) + 2O(C_{s_2})$ primitive Pythagorean triples $\mathcal{P}_{s_2}^\circ$ from \mathcal{P}_{t+2o}° , and so on. The child vertices \mathcal{V}_r are handled as in the algorithm for arbitrary trees in [Section 3.3](#). For a cycle $c \in \mathcal{C}_r$ at root r , we maintain the following properties: The first $L_{\rightarrow}(C_c) + 2O_{\rightarrow}(C_c)$ triples are reserved to the subcacti rooted at p_{\rightarrow} . The next two Pythagorean triples $(x_{\rightarrow}, y_{\rightarrow}, \ell_{\rightarrow})$ and $(x_{\leftarrow}, y_{\leftarrow}, \ell_{\leftarrow})$ are used for drawing p_{\leftarrow} and p_{\rightarrow} ; creating a parallelogram-shaped representation of c as detailed below if c is not a triangle; if c is a triangle, we also incorporate a single horizontal segment. Finally, the remaining $L_{\leftarrow}(C_c) + 2O_{\leftarrow}(C_c)$ triples are reserved for the subcacti rooted at p_{\leftarrow} .

Let $\rho_1^c, \dots, \rho_j^c$ denote the cut-vertices that are internal vertices along $p_{\rightarrow}(c)$, and let $\lambda_1^c, \dots, \lambda_i^c$ denote the cut-vertices along $p_{\leftarrow}(c)$ without s_c (it might be that $\lambda_i^c = t_c$). We



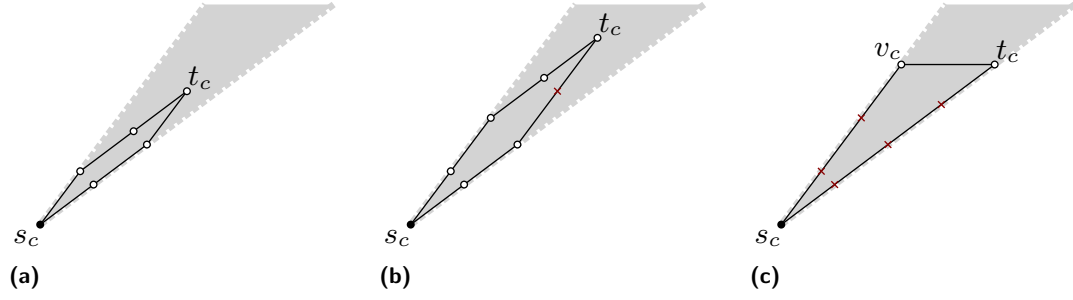
■ **Figure 5** Schematization of our recursive drawing algorithm in Section 3.4: Vertex r is placed at $(0,0)$ and its subtree is drawn inside the light-gray cone according to Invariant 2. Each of its successor components is assigned an exclusive set of slopes resulting in the non-overlapping gray cones centered at the child components. For child vertex v_i , the edge between r and v_i is drawn using the first triple assigned to v_i . For a child cycle c_j , two slopes are used to create either a parallelogram-shaped or triangle-shaped cycle. Subcacti rooted at cycles are assigned a subset of the slopes assigned to the cycle as indicated by the dark-gray cones.

assign the $L(C_c) + 2O(C_c)$ triples in order. First, we assign each ρ_k^c with $k \in \{1, \dots, j\}$ the required $L(C_{\rho_k^c}) + 2O(C_{\rho_k^c})$ triples in increasing order of k . The next two triples called $(x_{\rightarrow}, y_{\rightarrow}, \ell_{\rightarrow})$ and $(x_{\leftarrow}, y_{\leftarrow}, \ell_{\leftarrow})$, are not assigned to any child and instead used for drawing c . Finally, the remaining triples are assigned to each λ_k^c with $k \in \{1, \dots, i\}$, each subcactus gets the required $t(C_{\lambda_k^c}) + 2O(C_{\lambda_k^c})$ triples, but this time in decreasing order of k . The child components rooted at c contain in total one cycle less, thus, this assignment is valid. We use $\mathcal{P}(v)$ to denote the ordered set of primitive Pythagorean triples assigned to a vertex v .

Before we describe how to draw cycles, we discuss the recursion step, which is similar to Section 3.3. For each vertex $v \in \mathcal{V}_r$, draw C_v recursively with v as root, and for each cycle $c \in \mathcal{C}_r$ and each cut-vertex w in c where $w \neq s_c$, draw C_w recursively with w as root. As before, we use only the assigned triples for drawing edges inside subcacti; see also Figure 5.

Canonical drawing of cycles. Drawings of cycles occur both in the base case and in the recursive step, thus, we first discuss them independently. Let $(x_{\rightarrow}, y_{\rightarrow}, \ell_{\rightarrow})$ and $(x_{\leftarrow}, y_{\leftarrow}, \ell_{\leftarrow})$ denote the two triples assigned for drawing c such that $\alpha(x_{\rightarrow}, y_{\rightarrow}, \ell_{\rightarrow}) < \alpha(x_{\leftarrow}, y_{\leftarrow}, \ell_{\leftarrow})$, $p_{\leftarrow}(c) = (s_c = \lambda_1, \lambda_2, \dots, \lambda_i = t_c)$ and $p_{\rightarrow}(c) = (s_c = \rho_1, \rho_2, \dots, \rho_j = t_c)$. We assume, w.l.o.g., that s_c is placed at $(0,0)$ and distinguish three cases depending on lengths i and j .

- $i = j$ (see also Figure 6a): In this case, $t_c = \lambda_i = \rho_j$. Starting from s_c , we draw $p_{\rightarrow}(c)$. Namely, for $2 \leq k < j$, we place ρ_k at position $(x_{k-1} + x_{\rightarrow}, y_{k-1} + y_{\rightarrow})$ where (x_{k-1}, y_{k-1}) denotes the position of ρ_{k-1} . Finally, we place t_c at $(x_{j-1} + x_{\rightarrow}, y_{j-1} + y_{\rightarrow})$. Then, we draw $p_{\leftarrow}(c)$ analogously. Namely, we place λ_2 at $(x_{\leftarrow}, y_{\leftarrow})$ and then, for $3 \leq k \leq i$, we place λ_k at position $(x_{k-1} + x_{\rightarrow}, y_{k-1} + y_{\rightarrow})$ where (x_{k-1}, y_{k-1}) denotes the position of λ_{k-1} . That is, on either path, we have one edge realized with $(x_{\leftarrow}, y_{\leftarrow}, \ell_{\leftarrow})$ and $i - 1$ edges realized with $(x_{\rightarrow}, y_{\rightarrow}, \ell_{\rightarrow})$. Thus, t_c occurs at the same position on each path.
- $i = j + 1$ and $j > 1$ (see also Figure 6b): Starting from s_c , we again first draw $p_{\rightarrow}(c)$. As previously, for $2 \leq k < j$, we place ρ_k at position $(x_{k-1} + x_{\rightarrow}, y_{k-1} + y_{\rightarrow})$ where (x_{k-1}, y_{k-1}) denotes the position of ρ_{k-1} . Finally, we place t_c at $(x_{j-1} + 2 \cdot x_{\rightarrow}, y_{j-1} + 2 \cdot y_{\rightarrow})$. For $p_{\leftarrow}(c)$, we now first place λ_2 at $(x_{\leftarrow}, y_{\leftarrow})$ and then λ_3 at $(2 \cdot x_{\leftarrow}, 2 \cdot y_{\leftarrow})$. Then, we proceed



■ **Figure 6** Canonical drawings of a cycle c where i and j denote the lengths of paths $p_{\leftarrow}(c)$ and $p_{\rightarrow}(c)$, respectively. (a) $i = j$, (b) $i = j + 1$ and $j > 1$, (c) $i = 2$ and $j = 1$. Red crosses indicate endpoints of segments realized according to a primitive Pythagorean triple with no placed vertex.

as previously, i.e., for $3 \leq k \leq i$, we place λ_k at position $(x_{k-1} + x_{\rightarrow}, y_{k-1} + y_{\rightarrow})$ where (x_{k-1}, y_{k-1}) denotes the position of λ_{k-1} . That is, on either path, $i - 1$ edges are realized with $(x_{\rightarrow}, y_{\rightarrow}, \ell_{\rightarrow})$. Moreover, path $p_{\leftarrow}(c)$ has two edges realized with $(x_{\leftarrow}, y_{\leftarrow}, \ell_{\leftarrow})$, whereas path $p_{\rightarrow}(c)$ has one edge realized with the non-primitive Pythagorean triple $(2x_{\leftarrow}, 2y_{\leftarrow}, 2\ell_{\leftarrow})$. Thus, t_c occurs at the same position on each path.

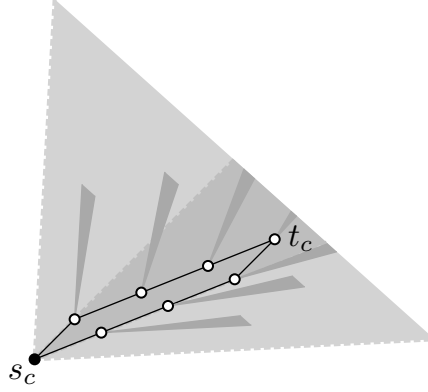
- $i = 2$ and $j = 1$ (see also Figure 6c): Here, c is triangle consisting of three vertices s_c , t_c and v_c . Let $Y_{\leftarrow} = \text{lcm}(y_{\leftarrow}, y_{\rightarrow})/y_{\leftarrow}$ and $Y_{\rightarrow} = \text{lcm}(y_{\leftarrow}, y_{\rightarrow})/y_{\rightarrow}$ where $\text{lcm}(y_{\leftarrow}, y_{\rightarrow})$ denotes the least common multiple of y_{\leftarrow} and y_{\rightarrow} . We place v_c at $(x_{\leftarrow} \cdot Y_{\leftarrow}, y_{\leftarrow} \cdot Y_{\leftarrow})$ and t_c at $(x_{\rightarrow} \cdot Y_{\rightarrow}, y_{\rightarrow} \cdot Y_{\rightarrow})$, i.e., we use the non-primitive Pythagorean triples $(Y_{\leftarrow} \cdot x_{\leftarrow}, Y_{\leftarrow} \cdot y_{\leftarrow}, Y_{\leftarrow} \cdot \ell_{\leftarrow})$ and $(Y_{\rightarrow} \cdot x_{\rightarrow}, Y_{\rightarrow} \cdot y_{\rightarrow}, Y_{\rightarrow} \cdot \ell_{\rightarrow})$ for drawing the edges (s_c, v_c) and (s_c, t_c) . The remaining edge (v_c, t_c) is horizontal since $y_{\leftarrow} \cdot Y_{\leftarrow} = \text{lcm}(y_{\leftarrow}, y_{\rightarrow}) = y_{\rightarrow} \cdot Y_{\rightarrow}$. Note that $\text{lcm}(y_{\leftarrow}, y_{\rightarrow}) \leq y_{\leftarrow} \cdot y_{\rightarrow}$.

We call the drawings constructed using the rules above the *canonical drawing* of a cycle c .

Properties of canonical drawings of cycles. It will be helpful to refer back to the following properties of canonical drawing of a cycle c , the first three of which are reminiscent of [Invariants 1–3](#) appearing in the correctness proofs for arbitrary trees and cacti below.

1. The drawing of c is a truly integral Fáry embedding with s_c at position $(0, 0)$.
2. The drawing of c lies in a cone that is rooted at v and bounded by two rays emanating at r and having slopes $y_{\rightarrow}/x_{\rightarrow}$ and $y_{\leftarrow}/x_{\leftarrow}$.
3. In the drawing of c , the Euclidean distance between s_c and any vertex v of c is at most $\left\lceil \frac{\text{len}(c)}{2} \right\rceil \cdot \frac{2\pi^2}{3} \cdot (t + 2o)$ if the length $\text{len}(c)$ of c is $\text{len}(c) \geq 4$. If $\text{len}(c) = 3$, the distances are at most $2 \left(\frac{\pi^2}{3} \cdot (t + 2o) \right)^2$.
4. Paths $p_{\leftarrow}(c)$ and $p_{\rightarrow}(c)$ are drawn monotone w.r.t. to a projection on the $(x_{\leftarrow}, y_{\leftarrow})$ - or $(x_{\rightarrow}, y_{\rightarrow})$ -direction. Moreover, no ray emanating from a point on $p_{\leftarrow}(c)$ of angle strictly greater than $\alpha(x_{\leftarrow}, y_{\leftarrow}, \ell_{\leftarrow})$ and no ray emanating from a point on $p_{\rightarrow}(c)$ of angle strictly smaller than $\alpha(x_{\rightarrow}, y_{\rightarrow}, \ell_{\rightarrow})$ intersects the drawing of c .
5. The rays emanating from s_c through the remaining vertices of c can be sorted increasingly according to slope as follows: $\overrightarrow{c\rho_1}, \overrightarrow{c\rho_2}, \dots, \overrightarrow{c\rho_j}, \overrightarrow{c\lambda_i}, \overrightarrow{c\lambda_{i-1}}, \dots, \overrightarrow{c\lambda_1}$.

It is easy to verify that Properties 1–4 are ensured by the construction; see also Figure 6. We are now ready include to cycles in the discussion of the base case and the recursive case.



■ **Figure 7** Schematization of the combination of child-components at a cycle.

Correctness. For establishing the correctness, we maintain the following invariants for each vertex v that is a cut-vertex, the root, or a leaf of C :

1. The drawing of C_v is a truly integral Fáry embedding.
2. The drawing of C_v lies in a cone that is rooted at v and bounded by two rays emanating at r and having slopes y_1/x_1 and $y_{L(C_v)+2O(C_v)}/x_{L(C_v)+2O(C_v)}$, where (x_1, y_1, ℓ_1) and $(x_{L(C_v)+2O(C_v)}, y_{L(C_v)+2O(C_v)}, \ell_{L(C_v)+2O(C_v)})$ denote the first and the last Pythagorean triple of $\mathcal{P}(v)$, respectively.
3. In the drawing of C_v , the Euclidean distance between v and any vertex of C_v is at most $(d(C_v) + O(C_v)) \cdot \frac{2\pi^2}{3} \cdot (t + 2o) + \Delta(C_v) \cdot 2 \left(\frac{\pi^2}{3} \cdot (t + 2o) \right)^2$.

Base Cases. There are two base cases for cacti. The first one is the leaf base case which we covered in [Section 3.3](#). The second one is a single cycle c with no child components – we use the canonical drawing of c . Properties 1–3 of the canonical drawing immediately imply [Invariants 1–3](#). In particular, observe that $\lceil \text{len}(c)/2 \rceil \leq d(c) + 1$ if $\text{len}(c) \geq 4$.

Recursion: Combining child components of a cut-vertex u . We consider the combination step where u is the root of C_u . Moreover, u has successor components $\mathcal{S}_u = \mathcal{C}_u \cup \mathcal{V}_u = \{s_1, \dots, s_k\}$ where \mathcal{C}_u is the set of child cycles with origin u and \mathcal{V}_u is the set of child vertices of u . We assume that we have drawn C_{s_1}, \dots, C_{s_k} according to [Invariants 1–3](#) and that if s_i (for $i \in \{1, \dots, k\}$) is a cycle it is already drawn in its canonical drawing using the slopes we assigned initially. We obtain a drawing for C_u by combining the drawings as follows.

First, we place u at $(0,0)$ and place the vertices $v \in \mathcal{V}_u$ using the first primitive Pythagorean triple of $\mathcal{P}(v)$ as in the previous case. Moreover, we add the canonical drawings of the child cycles $c \in \mathcal{C}_u$; recall that u is the origin of all of them. Then, for each cut-vertex w on a cycle c , we translate the recursively computed drawing of C_w to its position on c . Due to Property 1 for cycles and [Invariant 1](#) for recursively constructed subdrawings, all vertices of C_u are located on grid points and all edges of C_u have integer length. Thus, to obtain [Invariant 1](#), we have to ensure that there is no crossing in C_u . First, observe that the edges incident to u do not intersect and that cycles are plane according to Property 1. Second, assume that there is a crossing in the subdrawing of a child component. For \mathcal{V}_u , we can argue as in [Section 3.3](#). For $c \in \mathcal{C}_u$ observe the following: The slopes of edges in subcacti rooted on $p_{\leftarrow}(c)$ are steeper than the slope $y_{\leftarrow}/x_{\leftarrow}$ due to the assignment of triples discussed above. Similarly, the slopes of edges in subcacti rooted on $p_{\rightarrow}(c)$ are flatter than the slope

$y_{\rightarrow}/x_{\rightarrow}$. Thus, by Property 4 of the canonical drawing of c , the only possible intersections can be between two subgraphs rooted at $p_{\leftarrow}(c)$ or between two subgraphs rooted at $p_{\rightarrow}(c)$. For $p_{\rightarrow}(c)$, recall that the cut-vertices are monotone in $(x_{\rightarrow}, y_{\rightarrow})$ -direction. Moreover, the triples assigned to cut-vertices along $p_{\rightarrow}(c)$ are increasing in their angles (but having smaller angle than $(x_{\rightarrow}, y_{\rightarrow}, \ell_{\rightarrow})$. Therefore, no intersection is possible, as each subdrawing along $p_{\rightarrow}(c)$ uses flatter slopes than the succeeding ones, which complies with the sorting of rays $\overrightarrow{s_c p}$ as stated in Property 5; see Figure 7. Similarly, for $p_{\leftarrow}(c)$, recall that the cut-vertices are monotone in $(x_{\leftarrow}, y_{\leftarrow})$ -direction. Moreover, the triples assigned to cut-vertices along $p_{\leftarrow}(c)$ are decreasing in their angles. Therefore, no intersection is possible, as each subdrawing along $p_{\leftarrow}(c)$ uses steeper slopes than the succeeding ones, which complies with the sorting of rays as stated in Property 5; see Figure 7. Finally, intersections between different components with origin u are excluded due to Property 2 and Invariant 2.

For Invariant 2, the argument from Section 3.3 still applies as canonical drawings of cycles maintain Property 2 and we guarantee Invariant 2 for all recursively constructed drawings.

Finally, consider the maximum Euclidean distance between u and a vertex x in a subcactus rooted at $s \in \mathcal{S}_u$. For the child vertices, the argument is identical to Section 3.3 (using Invariant 2 for cacti). Hence, it remains to discuss the case where $s \in \mathcal{C}_u$. Let \mathcal{X}_c denote the cut-vertices on c except u . Then, due to Invariant 3 and Property 3, if $\text{len}(s) \geq 4$ we obtain:

$$\begin{aligned} \text{dist}(u, x) &\leq \left\lceil \frac{\text{len}(c)}{2} \right\rceil \cdot \frac{2\pi^2}{3} \cdot (t + 2o) + \\ &\quad \max_{w \in \mathcal{X}_c} \left((d(C_w) + O(C_w)) \cdot \frac{2\pi^2}{3} \cdot (t + 2o) + \Delta(C_w) \cdot 2 \left(\frac{\pi^2}{3} \cdot (t + 2o) \right)^2 \right) \\ &\leq (d(C_u) + O(C_u)) \cdot \frac{2\pi^2}{3} \cdot (t + 2o) + \Delta(C_u) \cdot 2 \left(\frac{\pi^2}{3} \cdot (t + 2o) \right)^2 \end{aligned}$$

If $\text{len}(s) = 3$, each subcactus rooted on c has at least one triangle less than C_u , and we get:

$$\begin{aligned} \text{dist}(u, x) &\leq 2 \left(\frac{\pi^2}{3} \cdot (t + 2o) \right)^2 + \\ &\quad \max_{w \in \mathcal{X}_c} \left((d(C_w) + O(C_w)) \cdot \frac{2\pi^2}{3} \cdot (t + 2o) + (\Delta(C_w) - 1) \cdot 2 \left(\frac{\pi^2}{3} \cdot (t + 2o) \right)^2 \right) \\ &\leq (d(C_u) + O(C_u)) \cdot \frac{2\pi^2}{3} \cdot (t + 2o) + \Delta(C_u) \cdot 2 \left(\frac{\pi^2}{3} \cdot (t + 2o) \right)^2 \end{aligned}$$

Thus, in either case we obtain Invariant 3. Invariants 1–3 for the root r imply Theorem 11.

► **Theorem 11.** *Let $C = (V, E)$ be a (rooted) cactus, which has n vertices, t leaves, diameter d , o cycles out of which δ are triangles. There is a truly integral Fáry embedding on a grid of size $\left(\frac{2\pi^2}{3} (d + o) (t + 2o) + \delta \cdot 2 \left(\frac{\pi^2}{3} \cdot (t + 2o) \right)^2 \right) \times \left(\frac{2\pi^2}{3} (d + o) (t + 2o) + \delta \cdot 2 \left(\frac{\pi^2}{3} \cdot (t + 2o) \right)^2 \right) \subseteq \mathcal{O}(n^3) \times \mathcal{O}(n^3)$, which can be found in $\mathcal{O}(n + (t + 2o)^{3/2})$ time.*

See Figure 8 for an example output. Note that for cacti with a constant number of odd cycles, we achieve area $\mathcal{O}(n^2) \times \mathcal{O}(n^2)$ as we did in the case for trees. If in addition, the diameter d is logarithmic, we once more achieve a grid size of $\mathcal{O}(n \log n) \times \mathcal{O}(n \log n)$.

4 Concluding Remarks and Open Problems

Our $\mathcal{O}(n^{3/2})$ -time algorithms become linear-time algorithms if we are given the Pythagorean triples instead of computing them from scratch every time. We conclude with open questions:



■ **Figure 8** Example output of our algorithm for general cacti. Observe the area blowup caused by the two triangular cycles.

1. Is Harborth's conjecture true for all planar graphs?
2. Provide an area lower bound for truly integral Fáry embeddings for binary trees. We conjecture that these require $\Omega(n^2)$ area. What is the lower bound for truly integral Fáry embeddings of (general) trees and cacti?
3. Compute area upper bounds for truly integral Fáry embeddings of other graph classes, e.g., more general graphs of treewidth two, like outerplanar graphs, or planar graphs of maximum degree four.
4. Are Harborth's and Kleber's conjectures equivalent? What if we require polynomial area for truly integral Fáry embeddings?

References

- 1 Vladimir I. Benediktovich. On rational approximation of a geometric graph. *Discret. Math.*, 313(20):2061–2064, 2013. doi:10.1016/J.DISC.2013.06.018.
- 2 T.G. Berry. Points at rational distance from the vertices of a triangle. *Acta Arithmetica*, LXII(4):391–398, 1992. doi:10.4064/aa-62-4-391-398.
- 3 Therese Biedl. Drawing some planar graphs with integer edge-lengths. In Greg Aloupis and David Bremner, editors, *Proc. 23rd Annual Canadian Conference on Computational Geometry (CCCG 2011)*, 2011. URL: <http://www.cccg.ca/proceedings/2011/papers/paper36.pdf>.
- 4 Daniel J. Chang and Timothy Sun. Harborth’s conjecture for 4-regular planar graphs. In Stefan Felsner and Karsten Klein, editors, *Proc. 32nd International Symposium on Graph Drawing and Network Visualization (GD 2024)*, pages 38–1. Schloss Dagstuhl–Leibniz-Zentrum für Informatik, 2024. doi:10.4230/LIPICS.GD.2024.38.
- 5 Norishige Chiba, Tadashi Yamanouchi, and Takao Nishizeki. Linear algorithms for convex drawings of planar graphs. *Progress in graph theory*, pages 153–173, 1984.
- 6 Hubert De Fraysseix, János Pach, and Richard Pollack. How to draw a planar graph on a grid. *Combinatorica*, 10(1):41–51, 1990. doi:10.1007/bf02122694.
- 7 István Fáry. On straight line representation of planar graphs. *Acta Sci. Math.(Szeged)*, 11:229–233, 1948.
- 8 Jim Geelen, Anjie Guo, and David McKinnon. Straight line embeddings of cubic planar graphs with integer edge lengths. *Journal of Graph Theory*, 58(3):270–274, 2008. doi:10.1002/jgt.20304.
- 9 Ronald L. Graham, Donald E. Knuth, and Oren Patashnik. *Concrete Mathematics: A Foundation for Computer Science*. Addison-Wesley, 1989. doi:10.1063/1.4822863.
- 10 Heiko Harborth, Arnfried Kemnitz, Meinhard Möller, and Andreas Süssenbach. Ganzzahlige planare Darstellungen der platonischen Körper. *Elem. Math.*, 45(5):118–122, 1987.
- 11 Goos Kant. Hexagonal grid drawings. In Ernst W. Mayr, editor, *Proc. 18th International Workshop on Graph-Theoretic Concepts in Computer Science (WG 1992)*, volume 657 of *Lecture Notes in Computer Science*, pages 263–276. Springer, 1992. doi:10.1007/3-540-56402-0_53.
- 12 Arnfried Kemnitz and Heiko Harborth. Plane integral drawings of planar graphs. *Discrete Mathematics*, 236(1-3):191–195, 2001. doi:10.1016/s0012-365x(00)00442-8.
- 13 Michael Kleber. Encounter at far point. *The Mathematical Intelligencer*, 30:50–53, 2008. doi:10.1007/bf02985756.
- 14 Ronald C. Read. *A new method for drawing a planar graph given the cyclic order of the edges at each vertex*. Faculty of Mathematics, University of Waterloo, 1986.
- 15 Walter Schnyder. Embedding planar graphs on the grid. In David S. Johnson, editor, *Proc. 1st Annual ACM-SIAM Symposium on Discrete Algorithms (SODA 1990)*, pages 138–148. SIAM, 1990. URL: <https://dl.acm.org/doi/10.5555/320176.320191>.
- 16 Wacław Sierpiński. *Pythagorean Triangles*, chapter 1. Primitive Pythagorean Triangles and 2. Obtaining Primitive Pythagorean Triangles, pages 1–10. Dover Publications, 2003.
- 17 Sherman K Stein. Convex maps. *Proceedings of the American Mathematical Society*, 2(3):464–466, 1951.
- 18 Timothy Sun. Rigidity-theoretic constructions of integral fary embeddings. In Greg Aloupis and David Bremner, editors, *Proc. 23rd Annual Canadian Conference on Computational Geometry (CCCG 2011)*, 2011. URL: <http://www.cccg.ca/proceedings/2011/papers/paper20.pdf>.
- 19 Timothy Sun. Drawing some 4-regular planar graphs with integer edge lengths. In Alejandro López-Ortiz, Therese Biedl, and Anna Lubiw, editors, *Proc. 25th Canadian Conference on Computational Geometry (CCCG 2013)*, 2013. URL: http://cccg.ca/proceedings/2013/papers/paper_47.pdf.
- 20 William Thomas Tutte. How to draw a graph. *Proceedings of the London Mathematical Society*, 3(1):743–767, 1963. doi:10.1112/plms/s3-13.1.743.
- 21 Klaus Wagner. Bemerkungen zum Vierfarbenproblem. *Jahresbericht der Deutschen Mathematiker-Vereinigung*, 46:26–32, 1936.